Optimum Design of a Packed Bed Reactor with Fluid Mixing : The Cases of a Parallel Reaction or a Successive Reaction

Optimum Design of a Packed Bed Reactor

with Fluid Mixing

— The Cases of a Parallel Reaction or a Successive Reaction —

Kenji Kubo*, Daisaburo Kato*

ABSTRACT

Optimum temperature profiles were computed along the axial direction of a packed bed flow reactor, by utilizing the distributed side mixing model for the description of non-ideal mixing characteristics. Computational procedure is used the maximum principle method and the method is compared with the method of steepest ascent. The reaction is adopted a parallel reaction and a successive one.

The finding is that, for large variance of residence time distribution, that is, for shallow bed condition, the optimal temperature profile calculated with the side mixing models are higher at near after the entrance of the reactor and lower at near before the exit than the optimum isothermal. By operating a reactor according to the optimum temperature profile with the distributed side mixing model, the length of reactor can be reduced.

Key words: Optimum design of reactor, optimum temperature profile, the distributed side mixing model, fluid mixing

1. Introduction

To design and control a thermal reactor with catalyst, the optimum temperature profiles along the reactor length are very important. Therefore, many investigators have been reported on the problem of optimal temperature profiles.

In connection with parallel reaction, $A \overset{\nearrow}{\underset{\searrow}{}} \begin{smallmatrix} B \\ C \end{smallmatrix}$, Takamatsu et al.[7,8] calculated the optimum temperature profiles of thermal reactor with the piston flow model and the C.S.T.R. as a model of fluid mixing in a reactor. Tichacek L.T.[10], Horns and Parish[4] are computed the optimal temperature profiles of reactor with one dimensional dispersion model. For a successive irreversible reaction, $A \to B \to C$, there are Fan's report[3] utilizing the piston flow model, Takamatsu's report[9] and Leung & Changs' report[6] using the one dimensional dispersion model as fluid mixing in the thermal catalyst reactor.

However, the piston flow model, the C.S.T.R. and the one dimensional dispersion model are unsatisfied as a model which describes accurately fluid mixing in a thermal catalyst reactor.

The distributed side mixing model (DSM model) with two parameters was made it clear to be better than the piston flow model, the C.S.T.R. and the one dimensional dispersion model as a fluid mixing model in packed bed type reactor by observation of flow pattern and measurement of residence time distribution in a reactor[1,2,5]. As the ground equations of the DSM model are very simple, so the model can be treated easily inspite of having two parameters. The model is applicable to more complex reactions.

In this paper, by utilizing the DSM model, the optimum temperature profiles which can be gotten the maximum yield of desired component at outlet of thermal reactor are computed for the cases of parallel and successive reactions, respectively.

2. Distributed Side Mixing Model [DSM Model]

Based on the photographic observation in voids and measuremet of residence time distribution in tube bundle and bead-packed beds, the fluid flow in beds is summarized as following three conditions.

(1) In the laminar region, the flow velocity observed at the center of flow passage differs noticeably from that at the surface of beads. This may explain why the faster flow causes a steep break-through of the residence time curve and slower flow causes the long tailing of the curve.

(2) In the transition region, the fluid in a void consists of a rapid flowing part and vortices. The unstable vortices are believed to cause the fluctuation of the residence time curve, and therefore may be a cause of the scattering of measured values of the axial dispersion coefficient.

(3) The packing arrangement affects the streamline and the shape of the residence time curve in the laminar and transition regions. The rhombohedral arrangement can reduce fluid stagnation, and hence the long tailing of the residence time curve and, consequently, the value of the effective axial dispersion coefficient.

By recomposing the results, the distributed side mixing model (illustrated in **Fig. 1**) is proposed as follows.

(1) The main flow of volume fraction $(1 - \beta)$ through the central part of each interstice of the packing is piston-like.

(2) There are side pockets of volume fraction β around the packing, in which complete mixing is assumed to occur only in the direction perpendicular to the main flow.

(3) There is a concentration difference between the main flow and the side pockets, which gives rise to mass transfer between the two regions. The resistance to such mass transfer, R_M, which we shall here call the side mixing resistance, is assumed to be concentrated at the boundaries between the region of main flow and the side pockets.

(4) The reaction proceeds not only in main flow

but also in side pockets. The rate of reaction in main flow is R_1 and that in side pockets is R_2.

The **DSM** model is simplified the Turner's side pockets model, it has two parameters β and M. β is the void fraction of side pockets and M is the side mixing factor. These parameters can be measured experimentally. β is calculated from the dead time of residence time curve, M is evaluated by relation $\bar{\tau}^2 = 2\beta^2/M$, where $\bar{\tau}^2$ is the variance of residence time distribution.
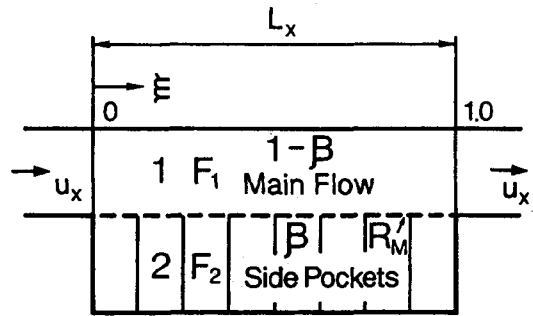

Fig. 1 Illustration of distributed side mixing model

3. Computation of Optimum Temperature Profile with Parallel Reaction

On the parallel first-order irreversible reaction, $A \underset{k_C}{\overset{k_B}{\rightleftharpoons}} {}^B_C$, it is the object to calculate the optimum temperature and concentration profiles which make to maximize the yield of B component at outlet of reactor ($\xi = 1.0$) with the **DSM** model.

Let pure substance of A be fed to the reactor inlet. The material balance equations are written as Eqs. (1), (2), (3) and (4). Where F_{1i} and F_{2i} are the mole fractions of the component i in the main flow and side pockets,

$$\frac{\partial F_{1A}}{\partial \xi} - M(F_{2A} - F_{1A})$$
$$+ (1 - \beta)(\frac{L_x}{U_x})(k_B F_{1A} + k_C F_{1A}) = 0 \quad (1)$$

$$M(F_{1A} - F_{2A}) - \beta(\frac{L_x}{U_x})(k_B F_{2A} + k_C F_{2A})$$
$$= 0 \quad (2)$$

$$\frac{\partial F_{1B}}{\partial \xi} - M(F_{2B} - F_{1B}) - (1 - \beta)(\frac{L_x}{U_x})k_B F_{1A}$$
$$= 0 \tag{3}$$

$$M(F_{1B} - F_{2B}) + \beta(\frac{L_x}{U_x})k_B F_{2A} = 0 \tag{4}$$

where M is the side mixing factor and β is the volume fraction of the side pockets.

The rate constants of reaction are all assumed to following Arrhenius' equation.

$$k_i = k_{i0} \, exp \, [-E_i/(R_g \cdot T)] \quad (i = B, C) \tag{5}$$

The boundary conditions at inlet are written as Eqs. (6) and (7).

$$F_{1A} = 1.0 \qquad at \quad \xi = 0 \tag{6}$$

$$F_{1B} = 0 \qquad at \quad \xi = 0 \tag{7}$$

F_{2A} and F_{2B} are rewritten as Eqs. (8) and (9) by utilizing Eqs. (2) and (4),

$$F_{2A} = \frac{MF_{1A}}{M + X(k_B + k_C)} \tag{8}$$

$$F_{2B} = F_{1B} + \frac{k_B}{M} F_{2A} X \tag{9}$$

where $X = \beta(L_x/u_x)$.

By substituting Eq. (8) into Eq. (1), Eq. (1) is rewritten as Eq. (10),

$$\frac{\partial F_{1A}}{\partial \xi} = [Y - \frac{MX}{M + X(k_B + k_C)}] (k_B + k_C)F_{1A} \tag{10}$$

where $Y = (1 - \beta)(L_x/u_x)$.

Equation (10) is solved with boundary condition of Eq. (6) and F_{1A} is given by Eq. (11),

$$F_{1A} = exp \, (-p\xi) \tag{11}$$

where $p = [Y - \frac{MX}{M + X(k_B + k_C)}] (k_B + k_C)$.

By utilizing Eqs. (8), (9) and (10), the required state equation of this process is derived as Eq. (12).

$$\frac{\partial F_{1B}}{\partial \xi} = k_B \, [\frac{M}{M + X(k_B + k_C)} - Y] \, exp \, (-p\xi) \tag{12}$$

Equation (12) is solved with boundary condition of Eq. (7) and then, F_{1B} is given by Eq. (13).

$$F_{1B} = \frac{\left\{ k_B \, [\frac{M}{M + X(k_B + k_C)} - Y] \right.}{P} \\ [1 - exp \, (-p\xi)] \left. \right\} \tag{13}$$

The Hamiltonian, $\mathbf{H}$, is given by Eq. (14).

$$\mathbf{H} = Z_1 \frac{\partial F_{1B}}{\partial \xi} \tag{14}$$

The optimal operating condition is given by partial differential of Hamiltonian Eq. (14) with temperature, T, and by equating it to be zero. That is;

$$\frac{\partial \mathbf{H}}{\partial T} = 0 \tag{15}$$

Equation (16) is derived from Eq. (15).

$$\xi = \frac{\left\{ (DKB) [\frac{M}{M + X(k_B + k_C)} - Y] \right.}{(DP)k_B [\frac{M}{M + X(k_B + k_C)} - Y]} \\ \frac{\left. -k_B \frac{M}{[M + X(k_B + k_C)]^2}(DK)X \right\}}{} \tag{16}$$

where

$$(DKB) = \frac{dk_B}{dT}, \quad (DK) = \frac{d(k_B + k_C)}{dT},$$

$$(DP) = \frac{dP}{dT}$$

Then, the concentration of B component at main flow can be obtained by substituting the values of ξ and T into Eq. (13).

4. Computational Results and Discussion of Parallel Reaction

Figures 2 and 3 show the computed optimum temperature and concentration profiles in the case of parallel reaction. For simplicity of calculation, it is assumed that the temperature in main flow part equal to that in side pockets. In order to compare the results of computation with that of other models, the kinetic data are cited. Kinetic data used to compute are listed in Table 1.
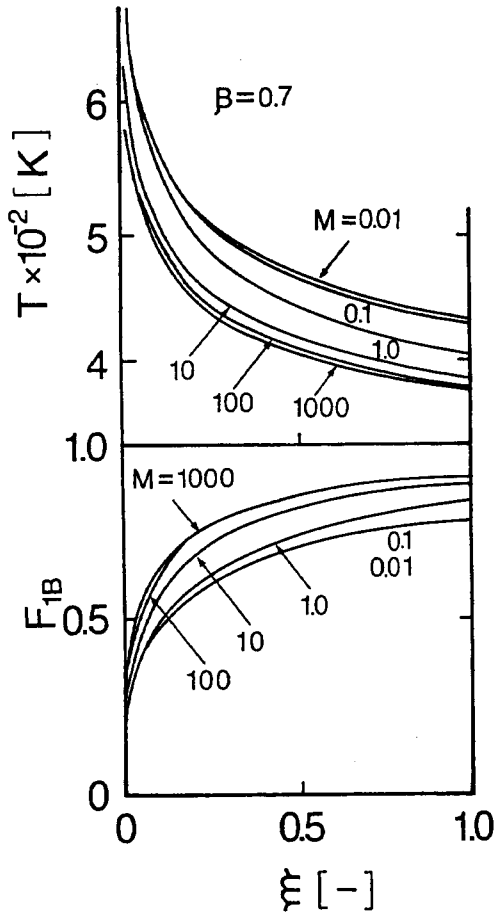
Fig. 2 Optimum temperature and concentration profiles with parallel reaction by letting β constant at 0.7.

Figure 2 shows optimum temperature, T, plotted as a function of dimensionless reactor

Table 1

Kinetic Data Used to Compute Figs. 2 and 3

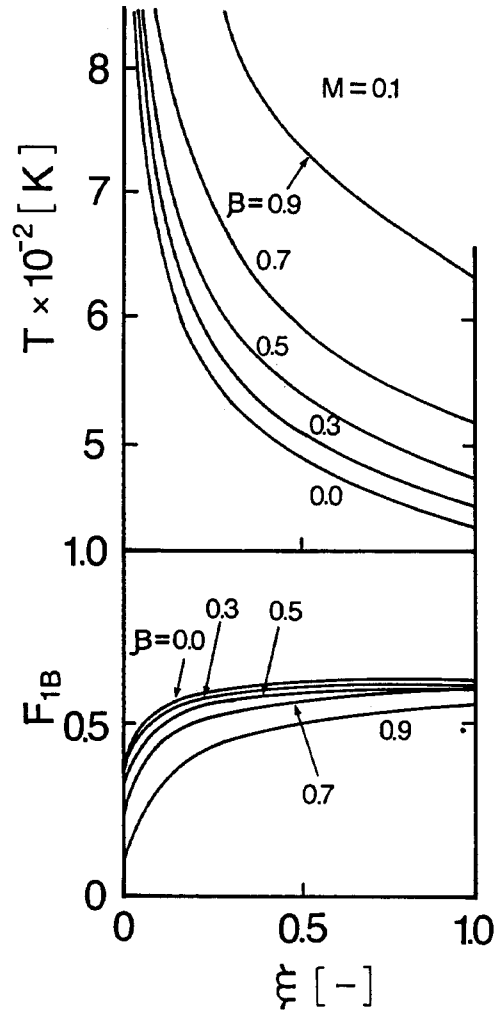|		
k_{BO}	62750	hr^{-1}
k_{CO}	502000	hr^{-1}
E_B	5559	cal/gmol
E_C	11120	cal/gmol
R_g	1.987	cal/gmol·K
L_x	3.048	m
u_x	304.8	m/hr

Fig. 3 Optimum temperature and concentration profiles with parallel reaction by letting M constant at 0.1.

length, ξ, for $M = 0.01, 0.1, 1.0, 10, 100$ and 1000 by letting β be constant at 0.7. Figure 3 also shows in the simillar manner for $\beta = 0.0$, 0.3, 0.5, 0.7 and 0.9 in the case M is constant at 0.1. The corresponding concentration profiles of the desired product are also plotted in Figs. 2 and 3. Yield at outlet of the reactor increase gradually in the value of M. When the value of M goes over 100, optimum temperature profiles are able to approximate that of piston flow. The lower the value of β becomes, the higher the yield of B component grows. When the value

of β is less than 0.1, optimum temperature profile is asymptotic to that of piston flow. For the purpose to attain higher yield, a reactor must be so designed as to increase the value of M, in selecting the shape of packing and flow condition. Pulsation of feed flow rate may also promote the mixing in the side pockets, therefore, can increase M.

5. Calculation of Optimum Temperature Profiles with Successive Reaction

On the successive first-order irreversible reaction, $A \xrightarrow{k_B} B \xrightarrow{k_C} C$, is considered. According to the above mensioned model, the equations of material balance for components A and B in main flow and in pockets are

$$\frac{\partial F_{1A}}{\partial \xi} = M(F_{2A} - F_{1A}) - (1 - \beta)(\frac{L_x}{u_x}) k_B F_{1A} \tag{17}$$

$$M(F_{1A} - F_{2A}) - \beta(\frac{L_x}{u_x}) k_B F_{2A} = 0 \tag{18}$$

$$\frac{\partial F_{1B}}{\partial \xi} = M(F_{2B} - F_{1B})$$
$$- (1 - \beta)(\frac{L_x}{u_x})(k_B F_{1A} - k_C F_{1B}) \tag{19}$$

$$M(F_{1B} - F_{2B}) + \beta(\frac{L_x}{u_x})(k_B F_{2A} - k_C F_{2B}) \tag{20}$$

Equation (21) is derived from (17), (18), (19), (20), and Arrhenius' equation (Eq. (5)),

$$\frac{\partial F_{1B}}{\partial \xi} + P F_{1B} = Q \exp(-Z \cdot \xi) \tag{21}$$

where

$$P = \frac{M k_C X}{M + k_C X} + k_C Y, \quad X = \beta(\frac{L_x}{u_x}),$$

$$Y = (1 - \beta)(\frac{L_x}{u_x}), \quad Q = \frac{M^2 k_B X}{(M + k_C X)^2} + k_B X,$$

$$Z = \frac{M k_B X}{M + k_B X} + k_B Y$$

The boundary condition at inlet are

$$F_{1B} = 0 \qquad \text{at} \quad \xi = 0 \tag{22}$$

$$F_{1A} = 1.0 \qquad \text{at} \quad \xi = 0 \tag{23}$$

By integrating from inlet to outlet of F_{1B} of ξ, F_{1B} is given as Eq. (24).

$$F_{1B} = \frac{Q}{P - Z} [\exp(-Z \cdot \xi) - \exp(-P \cdot \xi)] \tag{24}$$

The Hamiltonian, $\mathbf{H}$, is given by Eq. (25).

$$\mathbf{H} = Z_1 \frac{\partial F_{1B}}{\partial \xi} \tag{25}$$

The optimum temperature and concentration profiles are computed in the similar manner as mentioned above.

Computation with the method of steepest ascent is carried out as follows. The concentration of B component, F_{1B}, is expressed Eq. (24) as the function of dimensionless reactor length, ξ and temperature, T by utilizing the equations (17), (18), (19) and (20). The optimal temperature distribution is defined that which the concentration of desired component B makes maximum at exit of reactor. According to the method of steepest ascent, when $\Delta F_{1B}/\Delta \xi$ is selected to make maximum, the value of F_{1B} at outlet of reactor becomes to maximum. $\Delta \xi$ sets to constant at 0.01 and if the value of temperature at that point is assumed, $\Delta F_{1B}/\Delta \xi$ can be calculated through Eq. (24). This procedure is repeated as to increase $\Delta F_{1B}/\Delta \xi$ by correcting the value of T. Then, optimum temperature and concentration at that point are decided. The optimum temperature and concentration profiles are obtained by recurring these calculation from inlet ($\xi = 0$) to outlet ($\xi = 1.0$) of reactor.

6. Computational results and discussion of successive reaction

Figure 4 shows the optimum temperature and concentration profiles which are calculated for

Table 2

Kinetic Data Used to Compute Figs. 4 − 8

k_{BO}	3.21×10^{12}	hr^{-1}
k_{CO}	2.77×10^{19}	hr^{-1}
E_B	18000	cal/gmol
E_C	30000	cal/gmol
R_g	1.987	cal/gmol · K
L_x	3.048	m
u_x	22.86	m/hr
F_A ($\xi = 0$)	0.53	
F_B ($\xi = 0$)	0.43	

various values of β under the condition of $M = 0.1$. Whereas, **Figure 5** shows the effect of the M on these profiles by setting β be constant at 0.7. The kinetic data which utilize these calculation are the same Fan's data[3] as listed in **Table 2** for convenience of comparison. Comparing between Fig. 4 (optimum profiles of successive reaction) and Fig. 3 (optimum profiles of parallel reaction), two profiles are similar to each other. In the case of successive reaction, the smaller the value of β is, the lower the optimum temperature near after the entrance of reactor is and the higher the optimum temperature near before the outlet is. When the value of β decreases, the yield of desired component
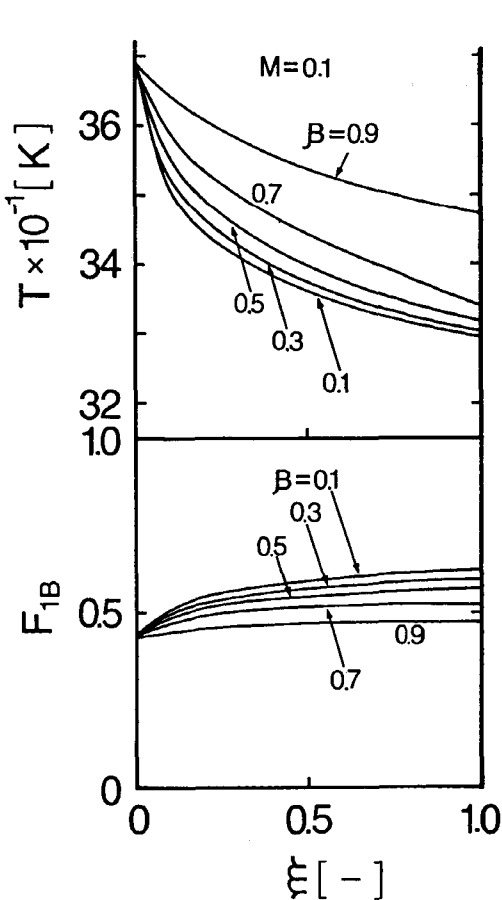

Fig. 4 Optimum temperature and concentration profiles with successive reaction by letting M constant at 0.1 (method of maximum principle)
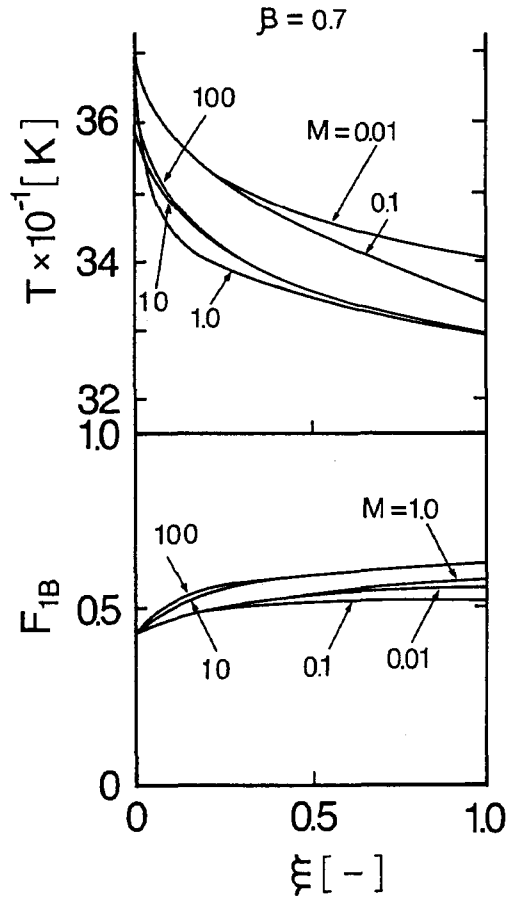
Fig. 5 Optimum temperature and concentration profiles with successive reaction by letting β constant at 0.7 (method of maximum principle)

increases. So, for getting to higher yield the value of $\bar{\tau}^2$ $(= 2\beta^2/M)$ is desired to reduce. Designning condition or operating condition which leads to increase in the volume of main flow need to obtain a good yield. Generally speaking, increase in M leads to higher yield. But, as shown in Fig. 5, when M is less than 1 the higher yield is achieved under the smaller value of M different from the case of parallel reaction. Accordingly, setting M to large value is not necessarily effectiveness for getting the higher yield under the lower value of M. However, when the value of M goes over 50 the variance becomes low value. In that case, the flow in the reactor is similar to

piston flow. The optimum temperature and concentration profiles of large value of M are the same as profiles of piston flow which were calculated by Fan[3].

Figures 6 and **7** show the optimum temperature and concentration profiles which are computed with the method of steepest ascent. The former is the case that M is constant and β changes, the latter is the opposit case, that is, β is constant and M is variable. Comparison these figures with Figs 4 and 5 (the profiles with the method of maximum principle) the optimum temperature with the method of steepest ascent is lower near after the inlet of reactor and higher near before the outlet. The yield which is cal-
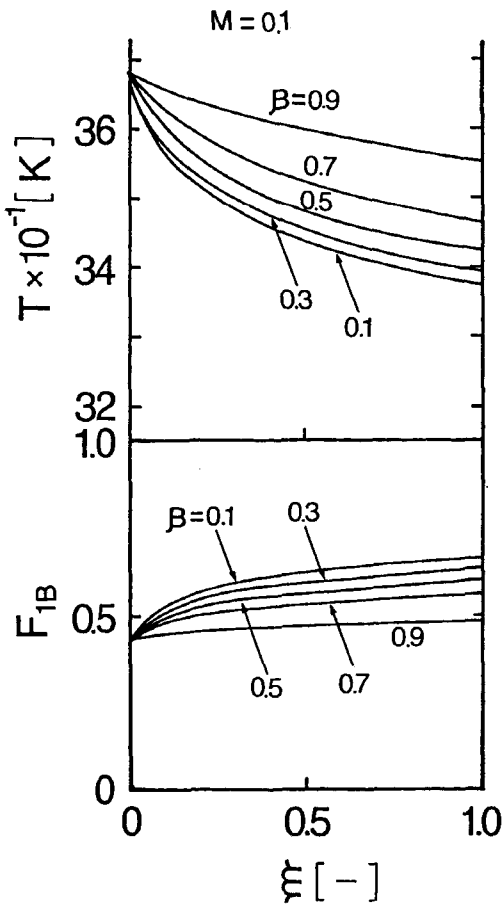

Fig. 6 Optimum temperature and concentration profiles with successive reaction by letting M constant at 0.1 (method of steepest ascent)
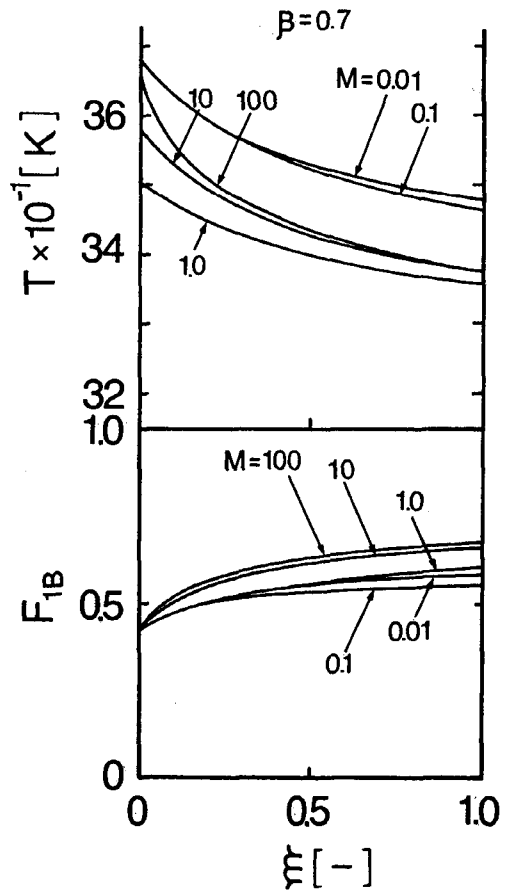
Fig. 7 Optimum temperature and concentration profiles with successive reaction by letting β constant at 0.7 (method of steepest ascent)

culated based on the method of steepest ascent is higher than that on the method of maximum principle. Particularly, in the case of large value of M, the difference between the two methods is expanded. When M is 100 the yield with the method of steepest ascent is higher 7% than that with the method of maximum principle. If the method of computation is different, the optimum temperature profile and concentration profile which are computed by the each method differ from each other. The maximum discrepancy between two methods attains 10%. Therefore, the discrepancy caused by the methods must be considered in study of the optimum design and optimum operation.

Figure 8 shows the optimum isothermal condition (constant temperature and concentration profile) which gives maximum yield computed
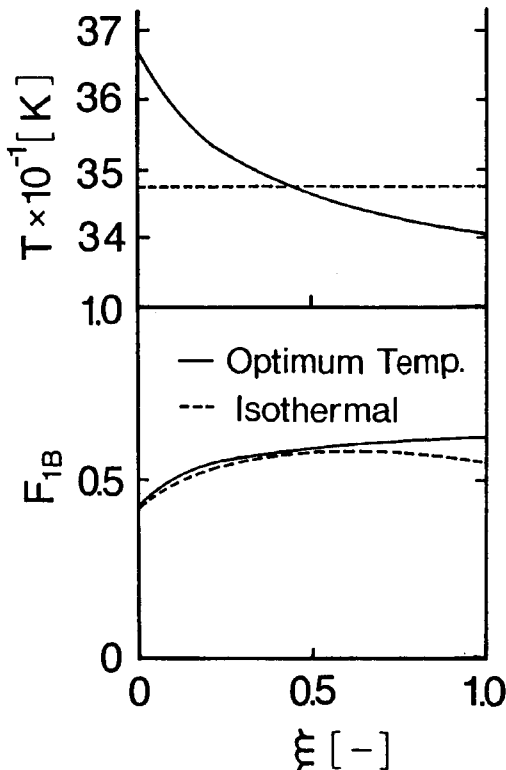

Fig. 8 Comparison of temperature and concentration between optimum condition and isothermal condition

by trial and error method. The optimum temperature profile with the method of steepest ascent is shown too in Fig. 8. The profile is that in the case of $M = 0.1$, $\beta = 0.3$ and $\bar{\tau}^2 = 1.8$, and that case is offen occurs in a packed bed type reactor. If the reactor is operated with optimum isothermal condition, the similar yield operated with optimum temperature profile is achived until the half of the reactor, but in the rest half the successive reaction proceeds over from component B to C so that the drop of yield at exit is noticed. In this case, the yield can be risen about 15% up by operating with the optimum temperature profile.

7. Conclusion

(1) The optimum temperature profiles computed with the distributed side mixing model is rather higher at immediately after the entrance of reactor and lower at near before the exit than the optimum isothermal. By operating the optimum temperature profile, the higher yield about 15% of desired component is attained comparison with that of the optimum isothermal.

(2) Packings or reactor should be designed or operated to make values of β as little, or make a value of M as large, as possible.

(3) The yield based on computation with the method of steepest ascent differs from that based on computation with the method of maximum principle. The maximum discrepancy between two methods is about 10%. Therefore, the discrepancy caused by procedure must be considered in discussion of the optimum design.

Nomenclature

E	= activation energy	[J/mol]
F	= concentration	[−]
$\mathbf{H}$	= Hamiltonian function	[−]
k	= rate constant	[1/s]
k_O	= frequency factor	[1/s]
L_x	= axial length of reactor	[m]
M	= side mixing factor ($= L_x/R_M u_x$)	[−]
R_g	= gas constant	[J/mol·K]
R_M	= side mixing resistance	[s]
T	= temperature	[K]
u_x	= interstitial linear velocity	[m/s]

< Greek letter >

β = volume fraction of side pockets [$-$]
ξ = dimensionless axial length [$-$]
τ = dimensionless time [$-$]
$\overline{\tau}^2$ = variance of residence time distribution from the mean, in terms of τ, 2nd moment [$-$]

< Subscript >

1 = main flow
2 = side pockets
A = component A
B = component B
C = component C

References

(1) Aratani T., K. Kubo, A. Misima and T. Yano, Journal of Chem. Eng. of Japan, **9**, 334 (1976).

(2) Aratani T., K. Kubo, A. Misima and T. Yano, Bull. Univ. Osaka Pref. **25**, 37 (1976).

(3) Fan L.T., The Continuous Maximum Principle (1966).

(4) Horns F.J.M. and T.D. Parish, Chem. Eng. Sci., **22**, 1949 (1967).

(5) Kubo K., T. Aratani, A. Misima and T. Yano, Chem. Eng. Journal, **18**, 209 (1949).

(6) Leung V. P. and K. S. Chang, A.I.Ch.E. Journal, **15**, 782 (1969).

(7) Takamatsu T., I. Hashimoto and F. Yoshida, Seigyo Kogaku (Japan), **13**, 664 (1969).

(8) Takamatsu T., I. Hashimoto and F. Yoshida, System and Control (Japan), **17**, 113 (1973).

(9) Takamatsu T., I. Hashimoto and Y. Sawanoi, Seigyo Kogaku (Japan), **11**, 469 (1967).

(10) Tichacek L. T., A.I.Ch.E. Journal, **9**, 394 (1963).